

more successful than the reactions with 4-tolylcopper(I) because of the increased stability of the mixed organo-(benzoato)copper(I) intermediates in the mesityl case.

The copper(I) 2-halobenzoates (halo is Cl or Br) synthesized via this method show similar IR spectra and reactivity toward mesitylcopper(I) as copper(I) benzoate, thus forming trimeric mixed (2-halobenzoate)organo-copper(I) clusters. Consequently, it is assumed that the structural features of these compounds are essentially similar. This means that the enhanced polarization of the carbon-halogen bond, by intramolecular coordination of the halogen to copper, which is proposed in the Hurtley reaction (see Scheme I), is not present in the pure copper(I) 2-halobenzoates $[\text{Cu}(\mu\text{-O}_2\text{CC}_6\text{H}_4\text{Cl-2})_4]$ (**1b**) and $[\text{Cu}(\mu\text{-O}_2\text{CC}_6\text{H}_4\text{Br-2})_4]$ (**1c**). However, under the conditions of the Hurtley reaction there are more species present than in our synthetic procedure and the temperature is considerably higher. The influence of all these factors will be discussed in a forthcoming paper.¹⁸

Finally, it should be emphasized that the reaction of copper(I) benzoates with arylcopper(I) compounds, which

generates mixed (benzoato)organo-copper(I) clusters, seems to be of a general nature.

Acknowledgment. These investigations were supported by the Netherlands Technology Foundation (S. T.W.). Andeno B.V. (Venlo) is thanked for stimulating this project. Prof. dr. K. Vrieze is thanked for his stimulating interest and Dr. D. M. Grove for critically reading the manuscript.

Registry No. **1a**, 62914-01-6; **1b**, 121619-88-3; **1c**, 121619-89-4; **2a**, 101997-12-0; **2b**, 122382-50-7; **2c**, 122382-51-8; **3a**, 122382-52-9; **3c**, 122382-53-0; Cu_5Me_5 , 88760-64-9; 2- $\text{ClC}_6\text{H}_4\text{CO}_2\text{H}$, 118-91-2; 2- $\text{BrC}_6\text{H}_4\text{CO}_2\text{H}$, 88-65-3; 2- $\text{MeC}_6\text{H}_4\text{CO}_2\text{H}$, 118-90-1; 2,4,6- $\text{Me}_3\text{C}_6\text{H}_2\text{CO}_2\text{H}$, 480-63-7; 2- $\text{NO}_2\text{C}_6\text{H}_4\text{CO}_2\text{H}$, 552-16-9; $\text{NCCH}_2\text{CO}_2\text{H}$, 372-09-8; $[\text{Cu}(\mu\text{-B}_2\text{C}_6\text{H}_4\text{Me-2})_n]$, 64508-54-9; $[\text{Cu}(\mu\text{-B}_2\text{CC}_6\text{H}_2\text{Me}_3\text{-2,4,6})_n]$, 122382-48-3; $[\text{Cu}(\mu\text{-B}_2\text{CC}_6\text{H}_4\text{NO}_2\text{-2})_n]$, 27269-44-9; $[\text{Cu}(\mu\text{-B}_2\text{CCH}_2\text{CN})_n]$, 122382-49-4; $\text{CuC}_6\text{H}_4\text{Me-4}$, 5588-74-9; $\text{C}_6\text{H}_5\text{CO}_2\text{H}$, 65-85-0.

Supplementary Material Available: Tables of isotropical parameters, anisotropical parameters, bond distances, and bond angles (7 pages); a listing of structure factors (9 pages). Ordering information is given on any current masthead page.

Fluxionality of $(\eta^2\text{-Naphthalene})(\text{Pr}_2\text{P}(\text{CH}_2)_n)_2\text{Ni}^0$ ($n = 2, 3$) in the Solid State and Solution As Studied by CP/MAS and 2D ^{13}C NMR Spectroscopy

Reinhard Benn,* Richard Mynott, Ivana Topalović, and Fred Scott†

Max-Planck-Institut für Kohlenforschung, Kaiser Wilhelm Platz 1, D-4330 Mülheim a. d. Ruhr, West Germany

Received December 23, 1988

Variable-temperature one- and two-dimensional liquid-state $^{13}\text{C}\{^1\text{H}\}$ and $^{31}\text{P}\{^1\text{H}\}$ spectra and solid-state MAS ^{31}P and CP/MAS ^{13}C NMR spectra of microcrystalline $(\text{C}_{10}\text{H}_8)(\text{dipp})\text{Ni}$ (**1**) and $(\text{C}_{10}\text{H}_8)(\text{dippe})\text{Ni}$ (**2**) (dipp = 1,3-bis(diisopropylphosphino)propane; dippe = 1,2-bis(diisopropylphosphino)ethane) confirm that the structures of these complexes in both aggregation states are identical. The arene is η^2 -bonded to nickel. In both the liquid and the solid state the P_2Ni moiety moves between the 1,2- and 3,4-positions within one ring of the naphthalene, but this does not interchange the phosphorus atoms. In solution this process is intramolecular and has an activation barrier of less than 6 kcal/mol while high-temperature 2D chemical exchange CP/MAS experiments yield an activation energy of more than 23 kcal/mol in the solid. Two-dimensional magnetization transfer experiments on the dissolved molecules confirm that there are two further fluxional processes involving rotation and migration of the P_2Ni moiety around the 1,2-, 3,4-, 5,6-, and 7,8-positions of both six-membered rings. The activation barrier for the migration of the η^2 -bonded P_2Ni moiety in the bicyclic compound is approximately 15 kcal/mol.

Introduction

Numerous simple organometallic molecules undergo fast dynamic processes in solution so rapidly even at low temperatures that the range of slow exchange cannot be reached in high-resolution ^{13}C high-field NMR spectroscopy.¹ An unambiguous structure determination is then often not possible. Even if an X-ray analysis is available for such compounds, in many cases the question remains open whether the structures in both aggregation states are identical and whether the molecules are also fluxional in the solid state.

In such situations solid-state NMR spectroscopy² is a particularly attractive technique. First, low-temperature studies are not restricted by the viscosity or freezing point

of a solvent. Thus a slow-exchange limit occurring at very low temperatures should be reached more readily in the solid state although under such conditions it is by no means a routine experiment to rotate air- and moisture-sensitive samples at high speeds.³ Second, the activation barrier for a given process may become much higher in the solid state. Even if the exchange rate is so low at elevated temperatures that no line broadening is evident, recently introduced one-⁴ and two-dimensional⁵⁻⁷ techniques based

(1) Mann, B. E. In "Comprehensive Organometallic Chemistry", Wilkinson, G., Stone, F. G. A., Abel, E. W., Eds.; Pergamon: Oxford, 1982; Vol. 3, p 89f.

(2) Mehring, M. *Principles of High Resolution NMR in Solids*; Springer-Verlag: Berlin, 1983. Fyfe, C. A. *Solid State NMR For Chemists*; CFA: Guelph, Ontario, Canada, 1983.

(3) For reviews: cf. Yannoni, C. S. *Acc. Chem. Res.* **1982**, *15*, 201. Haw, J. F. *Anal. Chem.* **1988**, *60*, 559A.

(4) Caravatti, P.; Bodenhausen, G.; Ernst, R. R. *J. Magn. Reson.* **1983**, *55*, 88.

* On sabbatical leave from the Rand Afrikaans University, Department of Chemistry and Biochemistry, P.O. Box 524, Johannesburg 2000, R.S.A.

on incoherent transfer of longitudinal magnetization can be employed for monitoring chemical exchange processes. These techniques are particularly sensitive for detecting processes occurring at rates of the order of $\{T_1(^{13}\text{C})\}^{-1}$. Since $T_1(^{13}\text{C})$ in the solid state is usually several seconds to a few minutes,² these methods are most promising for the detection and monitoring of very slow chemical exchange.

An interesting class of compounds where the above-mentioned situation is encountered are bis(phosphine)-(arene)nickel complexes.⁸ According to the low-temperature solution ^1H and ^{13}C NMR spectra in $(\text{C}_{10}\text{H}_8)$ -(dipp)Ni (**1**) and $(\text{C}_{10}\text{H}_8)$ (dippe)Ni (**2**) (dipp = 1,3-bis(diisopropylphosphino)propane; dippe = 1,2-bis(diisopropylphosphino)ethane) the metal appears to be η^4 -bonded to the arene because, for example, in the ^{13}C NMR spectrum, just five naphthalene signals are observed, of which two are shifted to higher field as a result of the complexation to Ni. On the other hand the X-ray analysis clearly demonstrates that in the crystal naphthalene⁹ or anthracene¹⁰ is η^2 -coordinated to the bis(phosphine)nickel residue. In the following we report the study of the variable-temperature solid- and liquid-state NMR spectra of **1** and **2** undertaken to explain this apparent contradiction. From these data the structure of these compounds in both the solid state and the liquid state as well as their dynamic behavior can be deduced unambiguously.

Experimental Section

Materials. The general synthesis of (bis(phosphine))(arene)-nickel complexes was reported earlier.⁸ The details of the preparation of the compounds **1** and **2** along with some spectroscopic data and an X-ray analysis of **2** was described recently.⁹ For the ^{13}C and ^{31}P NMR investigations in solution standard 10- and 5-mm sample tubes containing concentrated solutions of **1** and **2** in $\text{THF}-d_6$ were employed. For the ^{13}C and ^{31}P solid-state experiments double bearing zirconium oxide rotors of 7-mm outer diameter were filled with microcrystalline material of **1** and **2**. For this purpose a special homebuilt vessel was used, which permits loading of the rotor under inert atmosphere even at low temperatures.¹¹

NMR Spectra. All solid-state spectra were recorded by using the standard accessory on a Bruker AM 200 spectrometer. The ^{13}C spectra were recorded by using high power proton decoupling and magic-angle spinning for line narrowing and cross polarization for sensitivity enhancement. Spinning rates were between 3000 and 4500 Hz. The 90° ^{13}C pulse was 5.3 μs , and the contact time was varied between 0.5 and 20 ms. Optimum signal enhancements were achieved with a contact time of 4 ms. In the experiments with interrupted proton decoupling¹³ the dephasing time was between 40 and 80 μs . The temperature was varied between 235 and 355 K using a temperature controller and nitrogen as driving and bearing gas. Calibration of the temperatures was performed with external rotors filled with samarium acetate tetrahydrate.¹² Referencing of the ^{13}C shifts (± 0.1 ppm) was achieved by using the absolute frequencies relative to the methylene carbon of adamantane $\delta_{\text{TMS}}(\text{CH}_2) = 38.4$. The ^{31}P MAS spectra were re-

Table I. ^{13}C NMR Data of **1** and **2** As Obtained from the CP/MAS and Solution NMR Spectra

carbon no.	solid state ($T = 300$ K)		solution ($T = 183$ K)	
	$\delta(^{13}\text{C})$	T_1, s	$\delta(^{13}\text{C})$	$J(\text{C,H}), \text{Hz}$
		1		
1	51.0	25	84.7	156
2	50.2		91.1	155
3	121.7	30		
4	126.3			
5	129.4		125.9	155
6	126.3		123.5	156
7	117.1	40		
8	126.3			
9	138.9	45	137.4	
10	133.0	30		
		2		
1	50.9	20	84.9 ^a	156
2	50.1		91.3	157
3	120.3	32		
4	125.7	26		
5	128.6	27	125.9	156
6	124.7	26	123.4	159
7	115.8	27		
8	125.7	26		
9	138.9	57	137.5	
10	132	61		

^aTwo $J(\text{C,P})$ couplings of 9.2 and 3.0 Hz between 193 and 253 K.

corded without cross polarization by using a repetition time of 30 s. The 90° (^{31}P) pulse was 5 μs . Referencing of the $\delta(^{31}\text{P})$ scale was performed by using $\delta(\text{H}_3\text{PO}_4) = 0$ as external standard.

The solution ^{13}C experiments were carried out at 75.5 MHz by using conventional acquisition and processing techniques. Signal assignment was based on the values of the chemical shifts and the $J(\text{C,H})$ coupling constants.

$T_1(^{13}\text{C})$ measurements on solid **1** and **2** were performed employing cross polarization using a modified inversion recovery sequence as used by Torchia.¹⁴ T_1 values are given for individual well-resolved carbons, where integration posed no problems. The error limit for the values listed in Table I is ± 4 s.

2D magnetization transfer experiments in the solid state were carried out by using the standard pulse sequences^{5,6,15} and absolute value mode presentation. Usually 64 FIDs for different evolution times were collected for a spectral width of 5500 Hz. The mixing time was varied between 4 and 15 s in separate experiments, and consequently high-power proton decoupling in this time interval could not be employed in any of these records. Two-dimensional magnetization transfer spectra were recorded at $T = 300, 346,$ and 355 K by using otherwise identical acquisition parameters except for the spinning rate which was reduced to 2000 Hz at $T = 300$ K in order to enhance the cross peaks stemming from spin diffusion. The assignment of individual cross peaks were made from unsymmetrized contour plots. Only for the final presentation (cf. Figures 3 and 4) was symmetrization used.

The two-dimensional magnetization transfer experiments for dissolved **2** were carried out at 75.5 MHz at $T = 243$ K. A total of 256 FIDs, each consisting of 8 scans, were collected for 5882 Hz spectral width in F_1 dimension. The mixing time was 0.3 s.

Activation Parameters. Rate constants k for the chemical exchange of individual carbons were obtained from the intensity of the cross peaks in the two-dimensional contour plots using the formula¹⁶

$$I_d/I_c = (1 - k\tau_m)/k\tau_m$$

where I_d and I_m denote the intensity of the diagonal and cross peaks and τ_m denotes the mixing time. From the Eyring equation

(14) Torchia, D. P. *J. Magn. Reson.* 1978, 30, 613.

(15) For a recent method enhancing carbon spin diffusion in magic-angle spinning experiments: cf. Colombo, M. G.; Meier, B. H.; Ernst, R. R. *Chem. Phys. Lett.* 1988, 146, 189.

(16) Cf. ref 7, p 492.

(5) Sutter, D.; Ernst, R. R. *Phys. Rev. B: Condens. Matter* 1982, 25, 6038.

(6) Szevereyi, N. M.; Sullivan, M. J.; Maciel, G. E. *J. Magn. Reson.* 1982, 47, 462.

(7) Ernst, R. R.; Bodenhausen, G.; Wokaun, A. *Principles of Nuclear Magnetic Resonance in One and Two Dimensions*; Clarendon: Oxford, 1987.

(8) Jonas, K. *J. Organomet. Chem.* 1974, 78, 273.

(9) Jonas, K.; Scott, F.; Krüger, C. *J. Organomet. Chem.*, to be submitted for publication.

(10) Brauer, D. J.; Krüger, C. *Inorg. Chem.* 1977, 16, 884.

(11) Grondey, H. Ph.D. Thesis, Universität Siegen, West Germany, 1988. Benn, R.; Grondey, H., to be submitted for publication.

(12) Campbell, G. C.; Crosby, R. C.; Haw, J. F. *J. Magn. Reson.* 1986, 69, 191.

(13) Opella, J. S.; Frey, M. H. *J. Am. Chem. Soc.* 1979, 101, 5854.

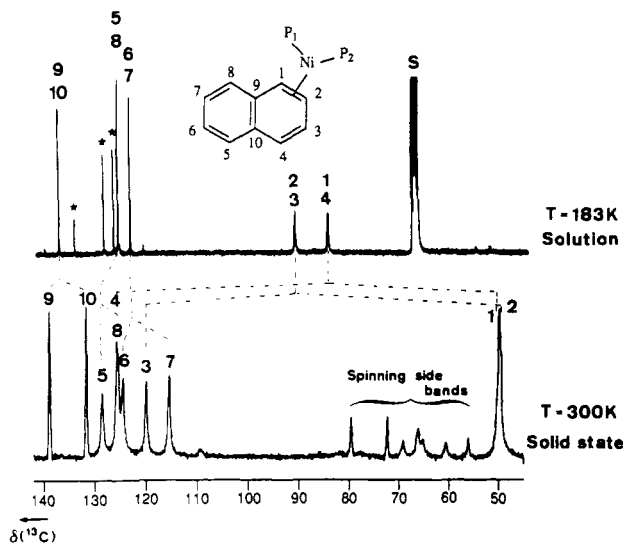


Figure 1. Arene signals in the ^{13}C NMR spectra of **2**. (a) CP/MAS spectrum at $T = 300$ K employing a spinning rate 3000 Hz. Signals for which mutual chemical exchange was observed at $T = 346$ K are marked by dotted lines. (b) $^{13}C\{^1H\}$ solution spectrum at $T = 183$ K. Signals indicated by asterisks stem from free naphthalene.

a lower limit for ΔG^\ddagger can then be obtained. From the low temperature solution spectra of **2** (fast-exchange limit) the rate constant k was obtained by using the equation $k = \pi(\Delta\nu)^2 / (2W_{1/2})$.¹⁷ Here $\Delta\nu$ is the shift difference between the two broadening sites in the slow-exchange limit as obtained from the solid-state spectrum, and $W_{1/2}$ is the half width of broadened line of the solution spectrum in the fast-exchange limit. The DNMR5 program¹⁸ was used for the calculation of exchange rates from the temperature-dependent ^{31}P spectra of **1** and **2** in solution in the temperature range from 223 to 300 K. The limits of error for the activation parameters are ± 0.8 kcal/mol.

Results and Discussion

Structure of 1 and 2 in the Solid State. The structure of complexes **1** and **2** in the solid state was derived from their ^{13}C CP/MAS NMR spectra, which exhibit well-resolved signals for the carbons of the arene and the phosphorus ligand (cf. Figure 1). There are two signals (each with the relative intensity 1) around $\delta(^{13}C) = 50$. They arise from two protonated carbons and are assigned to the complexed π -bond of the arene moiety. For these signals the coordination shift is about -75 ppm, a typical value for olefins complexed to late-transition-metal residues.¹⁹ The longitudinal relaxation times for these two signals are significantly shorter than those of the other ring carbon atoms. For **1** there are six additional distinct signals in the region typical for aromatic carbon atoms. Integration and plotting of the intensity of these signals versus different contact times²⁰ confirm that the shifts of three carbon atoms are isochronous and that the signals between 140 and 110 ppm in total belong to eight naphthalene carbon atoms. In the spectrum of **2** seven further signals are observed in the aromatic region since two are unresolved. The quaternary carbon atoms were readily identified by dipolar dephasing experiments.¹³

The resonances of the chelating ligand lying between 30 and 14 ppm were not all assigned unambiguously. The

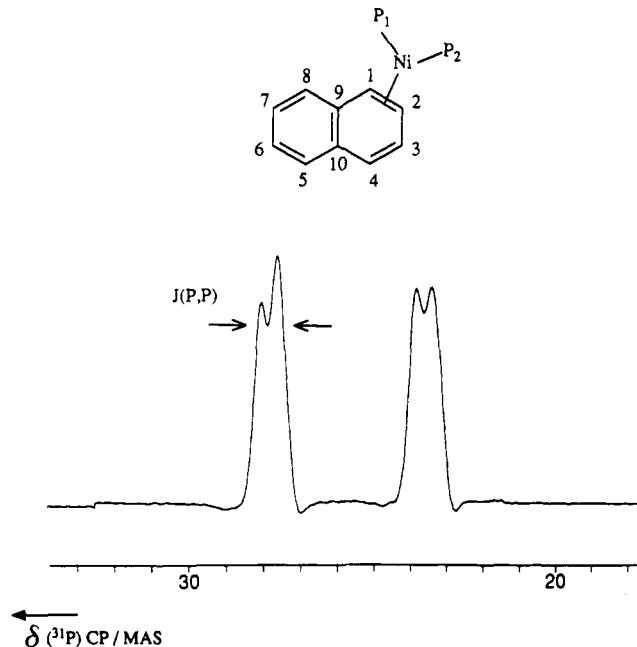


Figure 2. 81.0-MHz ^{31}P MAS spectrum of **1** employing a spinning rate of 3500 Hz. The scalar coupling $J(P,P)$ is resolved.

experiment with interrupted proton decoupling yields the signals for the methyl groups. In **1** the methylene carbons cannot be suppressed by these experiments, indicating that the chelating ligand undergoes fast conformational changes in the solid state even at $T = 243$ K. In **2**, however, the signals of the methylene carbons can be suppressed in the dipolar dephasing experiments at $T = 300$ K.

Since all carbon atoms in the naphthalene ligand in **1** and **2** are inequivalent and the carbon atoms bonded to nickel are protonated, this can only mean that the nickel is η^2 -bonded to the 1,2-positions of the arene, as already found for **2** in the single crystal.⁹ It is well-known from many examples,²¹ as well from the X-ray analysis of **2**,⁹ and from theoretical calculations²² that in quasi-trigonal moieties with a d^{10} electronic configuration like the olefin- NiL_2 complexes the coordinated double bond lies in the plane defined by Ni and the two phosphorus ligands.²³ Consequently it was not attempted to extract this information explicitly from the shielding tensors of the arene carbons.

According to the structural suggestions made above and in the absence of any chemical exchange process, the two phosphorus atoms in **1** and **2** are chemically inequivalent and this is confirmed by the ^{31}P MAS spectrum of **1** (cf. Figure 2). $J(P,P)$ as extracted from that spectrum is around $35 (\pm 5)$ Hz, which is in good agreement with the value (36.6 Hz) obtained in solution. Similar experiments were also carried out on **2**. Here we were not able to obtain a simple ^{31}P spectrum, most probably because a spinning rate of around 4500 Hz is insufficient to average out the dipolar phosphorus-phosphorus coupling in the five-membered chelating ring.

The full assignment of the arene signals in **1** and **2** (cf. Table I) is based on two-dimensional magnetization transfer^{5,6} experiments. Efficient exchange of longitudinal magnetization is achieved when the mixing period is about

(17) Günther, H. *NMR Spectroscopy*; Wiley: New York, 1980; p 243.

(18) Stephenson, D. S.; Binsch, G. DNMR5, Program 365 Quantum Chemistry Program Exchange, Indiana University, 1978.

(19) Mann, B. E.; Taylor, B. F. *^{13}C NMR Data For Organometallic Compounds*; Academic: New York, 1981.

(20) Harris, R. *Analyt* 1985, 10, 649.

(21) Harrison, N. C.; Murray, M.; Spencer, J. L.; Stone, F. G. A. *J. Chem. Soc., Dalton Trans.* 1978, 1337; cf. also ref 1.

(22) Albright, T. A.; Burdett, J. K.; Whangbo, M. H. *Orbital Interactions in Chemistry*; Wiley: New York, 1985.

(23) Krüger, C.; Tsay, Y. H. *J. Organomet. Chem.* 1972, 34, 387. Benn, R. *Org. Magn. Reson.* 1983, 21, 723.

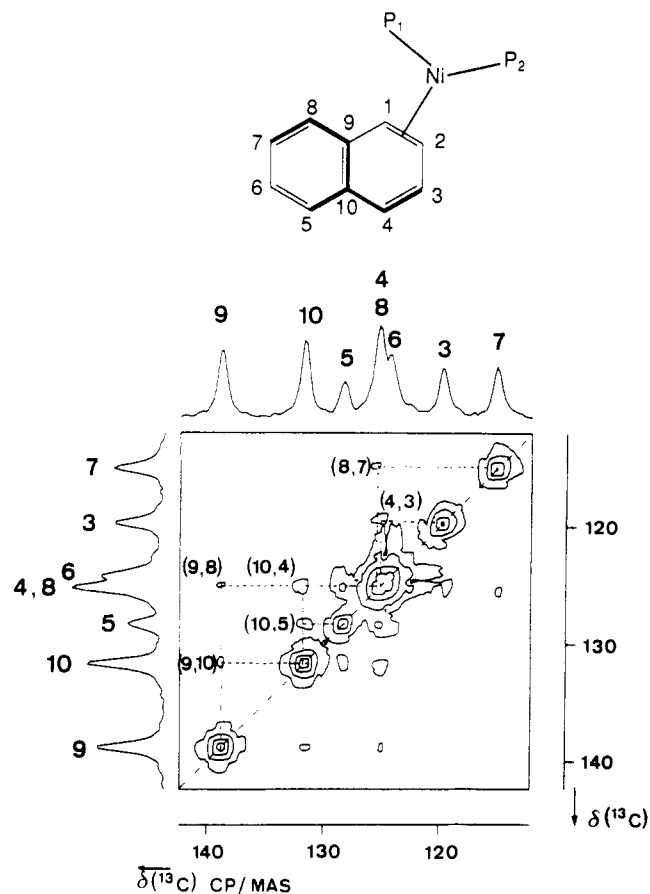


Figure 3. Contour plot stemming from a two-dimensional experiment on **2** at $T = 300$ K. Six cross peaks indicating spin diffusion are observed.

as long as $T_1(^{13}\text{C})$. Since the T_1 values of **1** and **2** at $T = 300$ K lie between 20 and 61 s, proton decoupling in the mixing period cannot be employed to discriminate between chemical exchange and spin diffusion.²⁴ To differentiate between these processes the variation of the intensity of the cross peaks with the temperature was monitored. Since in natural abundance samples it is unlikely that two magnetically active carbons are adjacent, cross peaks due to spin diffusion are of very low intensity. The formula that has most often been applied to describe the exchange probability W_{ij} per unit time in an isolated pair is²⁵

$$W_{ij} = 0.5\pi\omega_{ij}^2 F(0)$$

where ω_{ij} is the dipolar coupling between the two ^{13}C nuclei i and j and $F(0)$ is a factor describing the overlap of the uncoupled resonances $\delta(C_i)$ and $\delta(C_j)$, thus leaving in an MAS experiment besides ω_{ij}^2 the isotropic chemical shift difference as the relevant factor for the resonance overlap. It can be assumed that in complexes **1** and **2** in an ideal two-dimensional experiment involving extremely long mixing times τ_m , every arene carbon exhibits cross peaks with all the other ring carbons. In natural abundance samples the maximum intensity of these cross peaks, which may result from intra- and intermolecular interactions, should approach asymptotically 1% ($\tau_m \rightarrow \infty$). Although the details of the spin exchange in solids are complex, it can be assumed that it occurs most rapidly among nearby

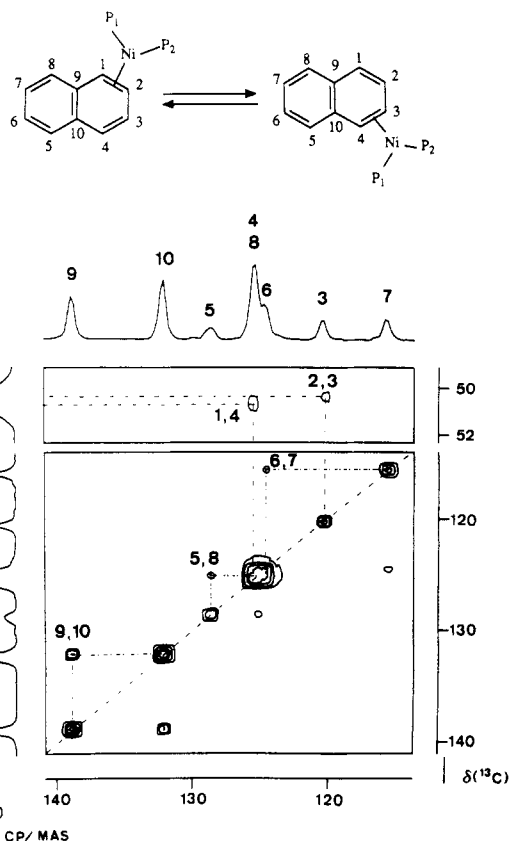


Figure 4. Expansions of the 50.3-MHz two-dimensional CP/MAS ^{13}C magnetization transfer spectra of **2** at $T = 346$ K. Note that although the two signals from the ring carbons C_1 and C_2 in the one-dimensional spectrum are not resolved, the corresponding signals in the two-dimensional experiment are clearly separated because of its intrinsic higher resolving power. The internal projections of the two-dimensional spectrum are presented on top and on the left-hand side.

nuclei. Opella and Frey have recently demonstrated that ^{13}C spin exchange at natural abundance can be used to probe very local structures in amino acids and polypeptides.²⁷ In the experiment illustrated in Figure 3 such a situation is also encountered. It is apparent that magnetization diffusion between adjacent carbons is the major process. There are 11 C–C bonds in the arene and consequently up to 11 pairs of cross peaks may arise by spin diffusion between nearest-neighbor carbon atoms. In the spectrum of **2** at $T = 300$ K six of these cross peaks were detected unambiguously even in the unsymmetrized two-dimensional contour plot. (Note that when the connectivities to the carbon atoms in the coordinated arene bond are neglected, only eight C–C bonds are left and that it is not clear whether there are also two additional cross peaks (stemming from magnetization diffusion between C_6 with C_5 and C_7 ; cf below)). The quaternary carbon at $\delta = 131$ shows three cross peaks connecting noncoordinated carbon atoms (C_4 , C_5 , C_9) and therefore is assigned to C_{10} . In agreement with this, C_9 has only two cross peaks in this region, which must arise from the noncoordinated carbons C_{10} and C_8 . Thus C_8 is identified. An additional cross peak from C_8 indicates the shift of C_7 . The unambiguous discrimination between C_4 and C_5 (cf. Figure 3) as well as the full assignment of the remaining arene carbon atoms (cf. Table I) becomes clear from the chemical exchange process, which is evidenced when the two-dimensional magnetization transfer experiment is carried out at $T =$

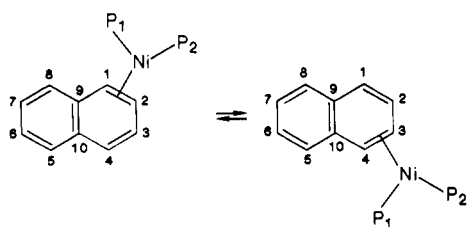
(24) Limbach, H.-H.; Wehrle, B.; Schlabach, M.; Kendrick, R.; Yanoni, C. S. *J. Magn. Reson.* 1988, 77, 84.

(25) Abragam, A. *The Principles of Nuclear Magnetism*; Oxford University: London, 1983; Chapter V, p 138 (paperback).

(26) VanderHart, D. L. *J. Magn. Reson.* 1987, 72, 13.

(27) Frey, M. H.; Opella, S. J. *J. Am. Chem. Soc.* 1984, 106, 4945.

Scheme I



346 K (cf. the section below, in particular Figure 4). These experiments give further support to the assignments made on the basis of the spin diffusion experiments. At the same time they show that it is generally not possible to detect C-C connectivities unambiguously by using the two-dimensional magnetization diffusion technique alone.

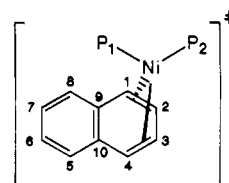
Structure in Solution. The liquid-state ^{13}C NMR spectra of 1 and 2 are quite different (cf. Figure 1b). There are only five resonances in the range from 140 to 80 ppm in the ^{13}C spectra of dissolved 1 and 2 at temperatures between 280 and 183 K. No signals are observed in the region around 50 ppm as have been found in the CP/MAS spectra of 1 and 2. Four of the signals are doublets while the remaining one at 137.4 ppm is a quaternary carbon. This suggests that the arene is η^4 -coordinated to the metal. However, in view of the X-ray structure and the solid-state spectra an alternative interpretation is that the ring is η^2 -bonded but possesses an element of symmetry due to a rapid chemical exchange process as illustrated in Scheme I.

The best indications that the naphthalene really is η^2 -coordinated in solution come from two facts: First, the chemical shifts are averages of the appropriate chemical shifts in the solid state. For example, the averages of C_8 and C_4 and of C_2 and C_3 in 1 and 2 lie between 85 and 90 ppm. This compares with chemical shifts around 85 and 90 ppm in solution. Second, at temperatures between 193 and 173 K the signals at ca. 91 and 85 ppm become broader than those at 137.5, 125.9, and 123.5 ppm. The broadening of the signals at 91 and 85 ppm is rationalized as resulting from a slowing down of the rate of exchange due to the process illustrated in Scheme I; the difference between the chemical shifts of the exchanging sites is greatest for C_1/C_4 and C_2/C_3 , and therefore these should show the effect of reducing the exchange rate earlier than the remaining signals.

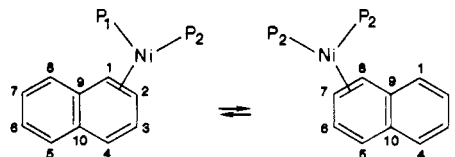
Dynamics of 1 and 2 in the Solid State and in Solution. Evidence for the exchange process occurring rapidly in solution even at 173 K can also be found in the solid-state spectra, though at much higher temperature. Analysis of the dynamic processes in 1 and 2 revealed in the solid state and solution NMR spectra shows that three aspects have to be considered. These are the 1,2 to 3,4 shift of the P_2Ni moiety in one ring of the naphthalene ligand, the exchange of the phosphorus atoms within the P_2Ni unit, and the shift of the P_2Ni moiety between the rings.

When the two-dimensional CP/MAS magnetization transfer experiments are carried out on 2 at $T = 346$ K, four cross peaks with much higher intensity are observed in addition to the cross peaks resulting from spin diffusion mentioned above. At the same time the cross peaks belonging to C_9 and C_{10} show a tenfold increase in intensity. The strong temperature dependence of these cross peaks shows that they must stem from a chemical exchange process. While the appearance of just five peaks in the 2D CP/MAS magnetization transfer spectrum in the solid state and the presence of five signals in the ^{13}C NMR spectrum in solution for the naphthalene ligand could be

Chart I



Scheme II



explained by a shift of the P_2Ni moiety from the 1,2-position to the 5,6-position, it is chemically more likely that it moves to the 3,4-position. (This interpretation is also supported by the fact that the two phosphorus atoms remain inequivalent during this process; cf. below.)

Once the nature of the exchange process has been established, the full assignment of the arene carbon signals can be completed with the help of the two-dimensional exchange spectrum. The second cross peak belonging to C_8 must stem from its exchange with C_5 . C_3 is identified by its cross peaks with C_4 in the 300 K spin diffusion spectra mentioned above, and C_6 is found by the cross peaks stemming from the chemical exchange with C_7 .

The rate constant for the exchange process according to Scheme I can be estimated from the intensity of the cross peaks and the mixing time. It is of the order of $2 \times 10^{-2} s^{-1}$ at $T = 346$ K, which yields for ΔG^\ddagger a value around 23 kcal/mol. Similar experiments carried out on 1 showed that the barrier for the isomerization process is about 2-4 kcal/mol higher than in 2. The temperature could not be raised enough to determine the activation parameters from a complete line-shape analysis because compounds 1 and 2 melted.

The barrier for the above-mentioned process in solution was estimated from the broadening of the signals at 91 and 85 ppm. At 193 K the additional line width is less than 15 Hz, and at 173 K it is less than 65 Hz for the one line and 47 Hz for the other. Assuming that the frequency differences between the two pairs of sites are 5630 Hz (75 ppm, corresponding to the shifts of 126 ppm for C_4 and 52 ppm for C_1 , cf. Table I) and 5300 Hz (70 ppm, corresponding to shifts of 121 ppm for C_3 and 51 ppm for C_2), then an upper limit of 5.4 kcal/mol can be placed on the barrier (cf. Experimental Section). This estimate depends only upon the magnitude of the shift difference and the broadening and is not critically dependent upon the exact values taken.

The sample contained a small quantity of free naphthalene, which yields sharp lines in the solution ^{13}C NMR spectra over the whole temperature range between 173 and 313 K. The free naphthalene therefore cannot be involved in the exchange process. Furthermore, two phosphorus couplings of 9.2 and 3.0 Hz to the naphthalene C_2 carbon atom are observed at 253 K, although the exchange process at this temperature is extremely fast. The naphthalene residue must therefore always remain bonded to the same P_2Ni moiety, and the exchange process must be intramolecular.

The 121-MHz ^{31}P spectrum of 1 dissolved in THF yields an AX pattern ($\Delta\nu = 500$ Hz) at temperatures below 223 K and a singlet at temperatures above 300 K. A line-shape analysis reveals that the barrier for the equivalencing

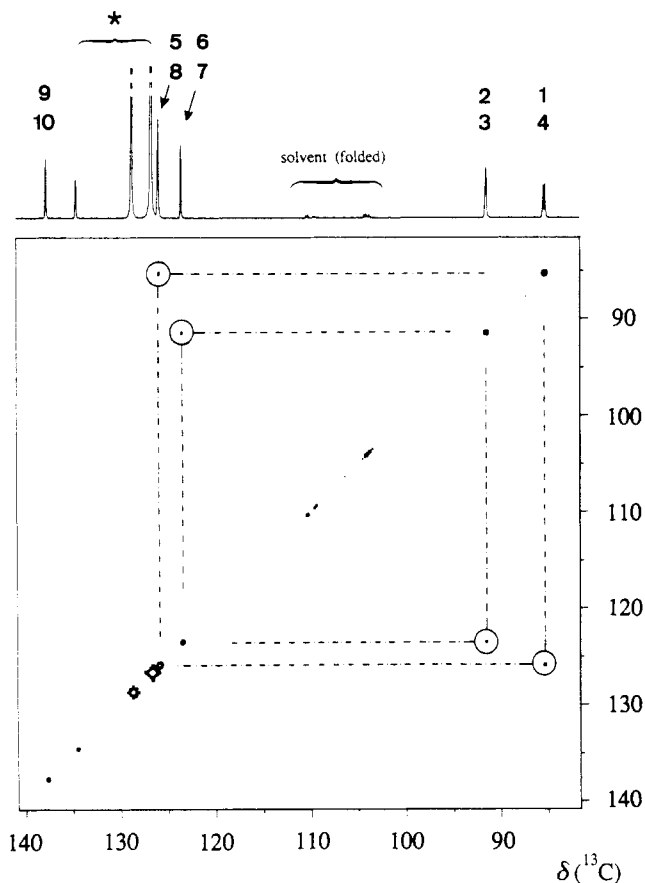


Figure 5. 75.5-MHz two-dimensional ^{13}C exchange spectrum of **2** at $T = 243\text{ K}$. The signals from free naphthalene are marked with an asterisk. Their intensities are greatly exaggerated because their line widths are much narrower and T_1 values are longer than of the corresponding carbon atoms in the complex. No cross peaks between the complexed and free naphthalene are observed.

of the two phosphorus atoms is 13 kcal/mol. Thus it must be concluded that in solution the exchange due to Scheme I, for which the barrier is much lower, proceeds by a process that does not interchange the phosphorus atoms. Therefore slipping of the PNiP fragment along the ring double bonds without its partial reorientation relative to the arene bonds (which would lead to a $(\eta^2\text{-arene})\text{NiP}_2$ transition state with the coordinated arene bond lying in the P-Ni-P plane) or dissociation can be excluded to account for this process. A process that is in agreement with all the spectroscopic information is a windshield wiper like motion of the PNiP moiety with an η^4 -coordination of C_1 , C_2 , C_3 , and C_4 of the arene as transition state (cf. Chart I). The barrier obtained for the phosphorus exchange lies close to that obtained for the rotation of the L_2Ni moiety about the ethylene in $\text{L}_2\text{Ni}(\eta^2\text{-C}_2\text{H}_4)$ complexes.^{22,23}

In solution at temperatures above 240 K a further exchange process takes place. This is evidenced by a broadening of the signals of the proton-bearing arene carbons. The two-dimensional exchange spectrum gives direct evidence for a pairwise equivalencing of the four doublet carbons (cf. Figure 5). This process can be rationalized as occurring by a movement of the PNiP moiety from the 1,2- or 3,4-position within the first ring to the 5,6-position and consequently also due to process 1 (cf. Scheme I) to the 7,8-position within the second arene ring (cf. Scheme II). For d^6 and d^8 ML_3 and $\text{M}(\eta^5\text{-Cp})$ fragments the reaction pathways of such haptotropic rearrangements in bicyclic polyene skeletons have been extensively investigated on the basis of extended Hückel MO

calculations.²⁸ For naphthalene complexes involving η^6 -bonded $\text{Cr}(\text{CO})_3$ and IrL_2^+ moieties the activation barrier for the haptotropic rearrangement has been determined experimentally.^{29,30} All these results show that the migration of $\text{Cr}(\text{CO})_3$ and isolobal fragments between the rings via a least motion pathway is symmetry forbidden and a circuitous route is preferred. To the best of our knowledge to date there are no previous reports of haptotropic inter-ring migrations of η^2 -bonded or d^{10} ML_2 moieties such as found in **1** and **2**.

Apparently the barrier to migration between the two rings of the naphthalene ligand is much lower for NiL_2 than for $\text{Cr}(\text{CO})_3$ moieties. From the intensity of the cross peaks in Figure 5 and the mixing time, the activation energy for this process was estimated to lie around 15 kcal/mol for **1** and **2**. An identical value was obtained by calculation of the rate constants from the line widths in the ^{13}C spectrum at 313 K. Movement of the L_2Ni moiety between the two naphthalene rings and its rotation around the coordination axis to the η^2 -bonded arene occur at much the same rate showing that activation barriers for the equivalencing of the phosphorus atoms and the exchange of rings in naphthalene are very similar. They may therefore be coupled processes or independent of one another.

We have not attempted to investigate the mechanism of the rearrangement illustrated in Scheme II. However, some conclusions can be directly drawn from the experiments presented in Figure 5. Since free naphthalene still gives sharp signals and furthermore there are no cross peaks connecting its carbon signals with those of the complex, it appears that this inter-ring migration process is also intramolecular. A direct proof for its being intramolecular from retention of the $J(\text{C,P})$ couplings was not possible since the line width of the signals of the protonated carbon atoms became too great to resolve these couplings and the sharp signals of the quaternary carbons showed no coupling to phosphorus at any temperature. The high-temperature limit could not be reached without the complex decomposing. The position of the averaged signal of the quaternary ring carbons is not shifted, so it can be concluded that population of a species in which the PNiP moiety is complexed to the $\text{C}_9\text{-C}_{10}$ bond is negligible.

Conclusion

We have shown that even from very air- and moisture-sensitive organometallic molecules highly resolved ^{13}C CP/MAS spectra can be obtained at various temperatures that allow a detailed structure elucidation of these complexes. These spectra facilitate and complement the interpretation of the solution ^{13}C NMR spectra. The two-dimensional magnetization transfer technique was found to be an extremely sensitive tool for the detection of dynamic processes in solid organometallic complexes. Moreover, we have illustrated that the problems associated with discrimination between chemical exchange and spin diffusion processes even on a relative elementary experimental level are not severe, at least for the molecules investigated here. Consequently we feel that the combination of high resolution liquid- and solid-state CP/MAS

(28) Albright, T. A.; Hofmann, P.; Hoffmann, R.; Lillya, C. P.; Dobosh, P. A. *J. Am. Chem. Soc.* **1983**, *105*, 3396.

(29) Kündig, E. P.; Perret, C.; Spichiger, S.; Bernadinelli, G. *J. Organomet. Chem.* **1985**, *286*, 183. Kündig, E. P.; Desobry, V.; Grivet, C.; Rudolf, B.; Spichiger, S. *Organometallics* **1987**, *6*, 1173. Oprunenko, Yu. F.; Malugin, S. G.; Ustynuk, Yu. A.; Ustynuk, N. A.; Kratsov, D. N. *J. Organomet. Chem.* **1988**, *338*, 357.

(30) Crabtree, R. H.; Parnell, C. P. *Organometallics* **1984**, *3*, 1727.

NMR techniques will become of wider interest for the comprehensive study of fluxional organometallic molecules.

Acknowledgments. F.S. thanks the Max-Planck-Gesellschaft for the grant of a stipend. R.B. thanks Prof. Dr.

K. Jonas for drawing his attention to the investigations of the haptotropic rearrangements mentioned in ref 28-30.

Registry No. 1, 121987-59-5; 2, 121987-60-8.

Photolysis of Tetracarbonylnickel in Dihydrogen-Containing Matrices: Evidence for the Formation of a Complex of Molecular Hydrogen

Ray L. Sweany,* Michael A. Polito, and Antoni Moroz

Department of Chemistry, University of New Orleans, New Orleans, Louisiana 70148

Received January 11, 1989

When H_2/Ar matrices of $Ni(CO)_4$ are irradiated by ultraviolet light, new infrared bands are detected that are assigned to a complex of molecular hydrogen, $Ni(CO)_3(H_2)$. The complex is characterized by two carbonyl stretching vibrations at 2033.1 and 2109.8 cm^{-1} . These bands and those of isotopically labeled molecules were used to calculate an anharmonic, energy factored force field with C_{3v} symmetry. The carbonyl stretching force constant of 1711.4 $N\cdot m^{-1}$ is intermediate between that of $Ni(CO)_4$ and $Ni(CO)_3$, an indication that the dihydrogen is probably coordinated as opposed to having been oxidatively added. The force field was used to calculate the OC-Ni-CO bond angle from the observed intensities of the carbon-12 isotopomer. The carbonyl portion of the molecule can be viewed as approximately tetrahedral, with the three remaining carbonyls more played than would be found in a tetracarbonyl complex. The angle between carbonyls is $115.6 \pm 1.0^\circ$. $Ni(CO)_3(H_2)$ loses H_2 with photons of the same energy as those which are used in its production. Thus, the quantity of $Ni(CO)_3(H_2)$ that could be formed was limited. None of the vibrational features that are associated with the hydrogen were observed by FTIR. This failure probably results from our inability to form large quantities of the complex and the inherent weakness of the hydrogen-containing vibrational modes. The hydrogen is probably bonded in an η^2 fashion in order for the H-H stretch to be so weak.

Introduction

Since the first published description of a complex of molecular hydrogen,¹ a number of complexes have been characterized, some of which are stable at room temperature.² Complexes of hydrogen have readily been formed in inert-gas matrices by the ultraviolet irradiation of stable 18-electron precursors in the presence of dihydrogen.³⁻⁵ Hydrogen concentrations as high as 25 mol % have been achieved in matrices. Thus, there is a high probability that every coordinatively unsaturated complex that is formed has at least one molecule of hydrogen nearby. Positive identification of the mode of bonding is made difficult because of the low intensity and broadness of some of the infrared modes which are most diagnostic, in particular, the H-H and the M-H₂ stretching modes of coordinated dihydrogen and the M-H stretching mode of a normal hydride.^{2,6} In previous matrix studies, and in this report, the behavior of the carbonyl modes are used to differentiate between hydrogen that has oxidatively added and that which has coordinated dihydrogen. Hydrogen withdraws less electron density from the metal when it coordinates than when it oxidatively adds, and the carbonyl modes can serve as a measure of this flow of metal electron

density. In extreme cases, it is easy to differentiate between the modes of bonding, although it is unclear how much a perturbation dihydrogen can cause and still be considered coordinated.⁴ Here, we report the formation of $Ni(CO)_3(H_2)$ in photolyzed matrices of $Ni(CO)_4$. An earlier report claiming the oxidative addition of hydrogen was based on early experiments in which a band was observed in the region of normal metal-hydride deformations.⁷ The observation of this band could not be repeated in subsequent experiments.

Results and Discussion

$Ni(CO)_3$ has been formed in matrices by the irradiation of $Ni(CO)_4$. Two absorptions were observed at 2067.4 and 2145.5 cm^{-1} .⁸ The relative intensity of the two modes vary considerably as a function of the matrix. Subsequently, the high-frequency band was shown to be due to near-neighbor interactions with other $Ni(CO)_4$ moieties.⁹ Only a single absorption was observed when $Ni(CO)_3$ was formed from Ni atoms and CO.¹⁰ Thus, $Ni(CO)_3$ can be presumed to be planar with only a single infrared-active carbonyl vibration. When H_2 is present in the matrix, two new bands at 2109.8 and 2033.1 cm^{-1} result from the irradiation of the matrix by 254-nm light. They are assigned to a new species which will be referred to as I. A typical spectrum

(1) Kubas, G. J.; Ryan, R. R.; Swanson, B. I.; Vergamini, R. J.; Waserman, H. J. *J. Am. Chem. Soc.* 1984, 106, 451-452.

(2) Kubas, G. J. *Acc. Chem. Res.* 1988, 21, 120-128.

(3) Sweany, R. L. *J. Am. Chem. Soc.* 1985, 107, 2374-2379.

(4) Sweany, R. L. *J. Am. Chem. Soc.* 1986, 108, 6986-6991.

(5) Sweany, R. L.; Russell, F. N. *Organometallics* 1988, 7, 719-727.

(6) Sweany, R. L.; Moroz, A. *J. Am. Chem. Soc.*, in press.

(7) Sweany, R. L. *Abstr. Pap., Am. Chem. Soc.* 1985, INOR 152.

(8) Rest, A. J.; Turner, J. J. *J. Chem. Soc., Chem. Commun.* 1969, 1026.

(9) Poliakov, M., unpublished results revealed in reviewer comments.

(10) DeKock, R. L. *Inorg. Chem.* 1971, 10, 1205-1211.